

# Chapter 24

## Imaging Presynaptic Exocytosis in Corticostriatal Slices

Minerva Y. Wong, David Sulzer, and Nigel S. Bamford

### Abstract

Optical imaging is a valuable tool for investigating alterations in membrane turnover and vesicle trafficking. Established techniques can easily be adapted to study the mechanisms of synaptic dysfunction in models of neuropsychiatric disorders and neurodegenerative diseases, such as drug addiction, Parkinsonism, and Huntington's disease. Fluorescent endocytic tracers, including FM1-43, have been used to optically monitor synaptic vesicle fusion and measure synaptic function in various preparations, including chromaffin cells, dissociated cell cultures, and brain slices. In this chapter, we describe a technique that provides a direct measure of pathway-specific exocytosis from glutamatergic corticostriatal terminals.

**Key words:** Optical, Imaging, FM1-43, ADVASEP-7, Multiphoton, Microscopy, Corticostriatal, Mouse, Electrophysiology

---

### 1. Introduction

Neurotransmitter release and reuptake from recycling synaptic terminals is tightly regulated and alterations in vesicular turnover or in the availability of neuromodulators that act presynaptically can be features of neurodegenerative conditions (1). Optical tracers that label individual axon terminals in an activity-dependent manner have become useful tools in neurobiology and are responsible for improving our understanding about membrane trafficking and synaptic activity. When combined with standard electrophysiological techniques, optical recordings enable synapse modeling by showing how neuromodulators select subsets of presynaptic terminals, leading to changes in postsynaptic activation.

Perhaps the first optical tracer to monitor neurotransmitter release used horseradish peroxidase, which in the presence of appropriate substrates can produce a colored or electron-dense

reaction product (2). Eric Holtzman showed that synaptic vesicles in lobster muscle accumulate and then release horseradish peroxidase upon stimulation (3), providing initial evidence that these organelles recycle and undergo multiple rounds of fusion with the plasma membrane.

Fluorophores were then adapted for endocytic labeling of synaptic vesicles, initially using Lucifer yellow in photoreceptors (4). Shortly after Jeff Lichtman and colleagues (5) used rhodamine, fluorescein, and 8-hydroxypyrene (which emit in red, green, and blue wavelengths, respectively) and stimulated multiple nerves innervating a neuromuscular junction to identify which axon terminals were associated with a particular nerve. Quantum dots have also been adapted for similar purpose (6). Additional classes of optical probes that have been used to study synaptic vesicle fusion are mutants of vesicle lumen proteins that possess pH sensitive mutant forms of green fluorescent protein (7). These “pHluorin” proteins have relatively low levels of emission in the typically acidic environment of synaptic vesicles, and become far brighter when exposed to the neutral extracellular milieu following fusion. Mutations of synaptic vesicle transporters are sometimes used as such tracers (8). Finally, fluorescent false neurotransmitters are accumulated by synaptic vesicle transporters, providing both a means by which destaining can be measured during exocytosis and a means to estimate vesicle accumulation under a range of circumstances (9).

To date, the most successful approach for studying the activity of corticostriatal terminals has been to use fluorescent styryl dyes, particularly FM1-43. This class of probes offers distinct advantages, including reversible staining, tissue impermeability and activated fluorescence when dissolved into the lipid bilayer membrane (10). These specialized qualities are bestowed by a positively charged head, which prevents membrane permeability, and a lipophilic tail of varying length that defines the dye’s spectral properties and washout kinetics (11). The compounds can also, like horseradish peroxidase, be used to form an electron dense reaction product (12) and a fixable derivative is available (13).

The FM dyes differ from other fluorescent tracers in that they are “amphiphilic” and can partition into membrane or aqueous media, but are most fluorescent when associated with lipid. Thus, the probe initially brightly labels the extracellular membrane. When neuronal stimulation induces endocytosis, the vesicle membrane becomes exposed to the synaptic cleft and FM1-43 is internalized within the recycling synaptic vesicle. When the synaptic vesicle membrane is endocytosed, FM1-43 fluorescence is visualized as bright fluorescent puncta. Restimulation produces exocytosis of recycling dye-loaded vesicles, FM1-43 is released into the extracellular medium or is dispersed in the surrounding membrane (14) and the fluorescence intensity of the terminal declines as it is desorbed from the membrane.

Preliminary evidence for the success of FM1-43 was demonstrated by William Betz and colleagues in frog, rat, and mouse motor nerve terminals (10). More recently, FM1-43 has been used to study secretory activity in chromaffin cells (11), cultured neurons (15, 16), as well as in hippocampal (17) and corticostriatal brain slices (18–21). Destaining of FM1-43 typically follows first to second order kinetics (15, 21) and is calcium dependent (18, 21), consistent with regulated neurotransmitter release.

An early identified impediment to using FM1-43 in brain slices was nonspecific “adventitious” binding of the dye that resisted washing and obscured the clear visualization of synaptic terminals. This problem was minimized following the introduction by Alan Kay of a carrier molecule, a sulfobutylated derivative of  $\beta$ -cyclodextrin, named ADVASEP-7 (22). This carrier was found to have a higher affinity for FM1-43 than plasma membranes and extracellular molecules, allowing for an efficient removal of FM1-43 from the extracellular space, and thus significantly reduced background staining. Additionally, two-photon laser-scanning microscopy (TPLSM) of FM1-43-labeled presynaptic terminals was found to be a superior method for visualizing dynamics of vesicle release and uptake (17, 23). Compared to confocal laser microscopy, TPLSM preserves tissue health by requiring less energy (at twice the wavelength), suppresses background fluorescence by membrane-bound FM1-43, increases the depth of excitation and leads to better imaging resolution of individual presynaptic boutons deep within a slice (24). Thus, we have found that optical imaging of presynaptic release in brain slices with FM1-43 is optimized by using TPLSM along with the external application of ADVASEP-7.

Here, we describe a technique that provides a direct measure of pathway-specific exocytosis from glutamatergic corticostriatal terminals. We provide instructions for loading FM1-43 into striatal terminals via nonspecific potassium-driven endocytosis and by pathway specific cortical stimulation. The instructions are tailored toward investigators with some experience in electrophysiology and knowledge of TPLSM function and tuning.

---

## 2. Materials

### 2.1. Media

1. Artificial cerebrospinal fluid solution (ACSF): 109 mM NaCl, 5 mM KCl, 35 mM NaHCO<sub>3</sub>, 1.25 mM NaH<sub>2</sub>PO<sub>4</sub>, 20 mM HEPES, 1 mM MgCl<sub>2</sub>, 2 mM CaCl<sub>2</sub>, and 10 mM glucose (pH 7.3–7.4, 295–305 mOsm; see Note 1).
2. High potassium (K<sup>+</sup>) ACSF: 74 mM NaCl, 40 mM KCl, 35 mM NaHCO<sub>3</sub>, 1.25 mM NaH<sub>2</sub>PO<sub>4</sub>, 20 mM HEPES, 1 mM MgCl<sub>2</sub>, 2 mM CaCl<sub>2</sub>, and 10 mM glucose (pH 7.3–7.4, 295–305 mOsm; see Note 1).

### **2.2. Equipment for Two-Photon Excitation Time-Lapse Imaging**

1. Zeiss LSM 510 NLO TPLSM equipped with a titanium-sapphire laser (excitation 810 nm/emission 650 nm; Carl Zeiss, Germany; see Notes 2 and 3).
2. Plan Fluor ×40 oil-immersion objective (NA 1.3; Zeiss).
3. IBM computer.
4. Software.
  - (a) LSM 510 Browser software (Zeiss).
  - (b) Image J (Wayne Rosband, National Institutes of Health, Rockville, MD).
  - (c) SigmaPlot (SPSS, Chicago, IL), Excel (Microsoft, WA) or another graphics software package.

### **2.3. Chemicals and Supplies**

1. FM1-43 (8 μM; *N*-[3-(triethylammonio)propyl]-4-(4-dibutylaminostyryl) pyridinium dibromide; Invitrogen, Carlsbad, CA). Protect from light (see Note 3).
2. ADVASEP-7 (CyDex, Overland Park, KS).
3. NBQX (10 μM; 2,3-dihydroxy-6-nitro-7-sulphamoylbenzo(f)-quinoxaline-2,3-dione; A.G. Scientific, San Diego, CA).
4. APV (50 μM; D-2-amino-5-phosphonovaleric acid; Sigma, St. Louis, MO).
5. CPCCOEt (40 μM; 7-(hydroxyimino) cyclopropanoic acid ethyl ester; Tocris Bioscience, Ellisville, MO).
6. RC-27 L slice incubation chamber (56 μL/mm; Warner Instruments, Hamden, CT).
7. Custom slice anchor (see Note 4).
8. Twisted tungsten bipolar electrode (22 mm; Plastics One, Roanoke, VA).
9. Tektronix R564B wave generator (Tektronics, Gaithersburg, MD).
10. Stimulation isolator (AMPI, Jerusalem, Israel).
11. S88 storage oscilloscope (Grass-Telefactor, West Warwick, RI).
12. Carbogen gas (95% O<sub>2</sub>, 5% CO<sub>2</sub>).

---

## **3. Methods**

Optical imaging of release from corticostriatal terminals is measured using the endocytic tracer FM1-43, which reports synaptic vesicle fusion activity at individual terminals, using techniques introduced previously (18–21). In brain slice preparations, TPLSM,

combined with the judicious use of the adventitious quencher ADVASEP-7, provides a high signal to noise ratio and excellent three-dimensional spatial resolution with minimal photo bleaching and photo damage (24).

### **3.1. Preparation of the Corticostriatal Slice**

1. Prepare 1 L of ACSF and perfuse with carbogen gas. Check pH and osmolarity.
2. Isolate 50 cc of the ACSF, bubble in carbogen and cool in an ice bath.
3. Anesthetize mice with nembutal 200 mg/kg i.p. or other agent prior to sacrifice.
4. Decapitate, rapidly remove the brain and sever the cerebellum.
5. Affix the caudal portion of the forebrain to a vibratome tissue holder using a few drops of cyanoacrylate glue and fill the holder with the prepared ice-cold ACSF.
6. Cut tissue using a vibratome into four to six 250  $\mu\text{m}$ -thick coronal sections, containing the cortex and striatum between bregma +1.54 and +0.62 (25).
7. Bisect each coronal section at the midline creating two half-sections, each containing a hemisphere and striatum (see Fig. 1); remove to a slice holding chamber filled with carbogenated ACSF at room temperature.
8. Allow slices to recover for at least 1 h prior to use.
9. Prepare the following solutions, store in foil-lined plastic containers and bubble with carbogen for a few min just prior to using.
  - (a) 8  $\mu\text{M}$  FM1-43, 10 cc in High  $\text{K}^+$  ACSF.
  - (b) 1 mM ADVASEP-7, 10 cc in ACSF.
  - (c) 100  $\mu\text{M}$  ADVASEP-7, 10 cc in High  $\text{K}^+$  ACSF.
  - (d) 8  $\mu\text{M}$  FM1-43, 10 cc in ACSF.
  - (e) 100  $\mu\text{M}$  ADVASEP-7, 500 cc in ACSF.

### **3.2. Preparation for Optical Imaging with FM1-43**

1. Activate and tune the TPLSM (see Subheading 2.2).
2. Place a single corticostriatal slice in the imaging chamber with the cortex facing the electrodes (see Fig. 1a). Place the slice anchor over the slice so that harp strings run parallel with the corticostriatal fibers. Perfuse with warmed ( $35^\circ\text{C}$ ) carbogenated ACSF at 2–3 mL/min.

### **3.3. Loading and Unloading FM1-43 Using High $\text{K}^+$**

1. Load FM1-43 nonspecifically into striatal terminals with high  $\text{K}^+$ .
2. Stop ACSF perfusion, close the suction, and remove most of the ACSF from the imaging chamber. Slowly add 2 ml of FM1-43 in high  $\text{K}^+$  ACSF (see Step 9a in Subheading 3.1) to the

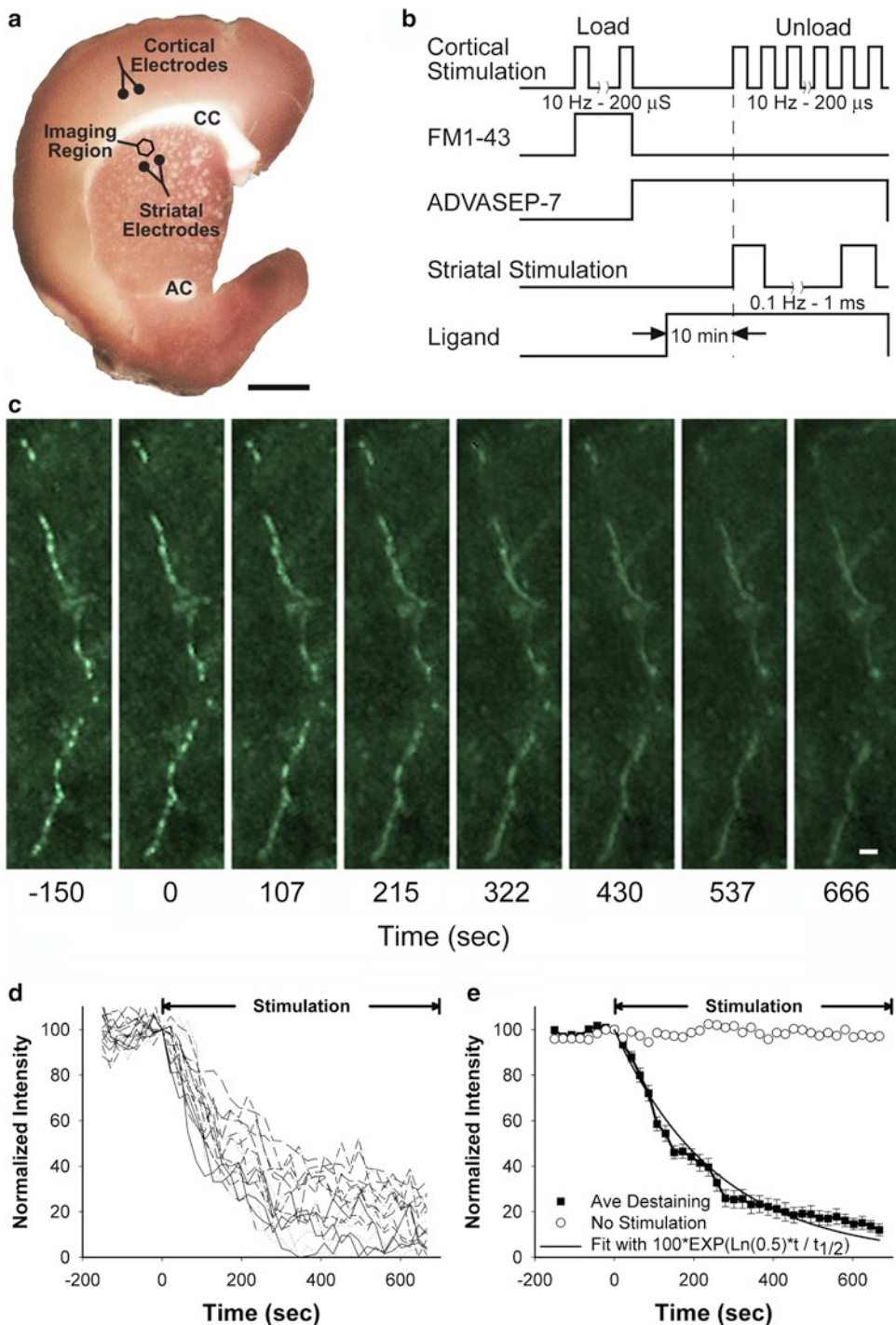


Fig. 1. (a) A corticostriatal slice stained with 3,3'-diaminobenzidine shows the areas of stimulation and recording. Corticostriatal terminals are loaded with FM1-43 by electrical stimulation with bipolar electrodes placed over cortical layers V–VI (Cortical Electrodes), located 1.5–2.0 mm from the imaging site. Multiphoton images of corticostriatal terminals are obtained from the corresponding motor striatum. Dopamine can be released by amphetamine or by local striatal stimulation (Striatal Electrode). CC corpus callosum, AC anterior commissure. Bar, 1 mm. (b) Protocol for loading and destaining corticostriatal terminals with FM1-43. (c) Multiphoton images of corticostriatal terminals captured every 21.5 s from the dorsal striatum revealed an *en passant* array of corticostriatal terminals. Restimulation at  $t=0$  with 10 Hz pulses shows activity-dependent destaining of fluorescent puncta. Bar, 2  $\mu$ m. (d) Time-intensity analysis of FM1-43 release from individual puncta ( $n=18$ ), shown in panel C, demonstrate diverse terminal kinetics. Stimulation began at  $t=0$  s. (e) Mean fluorescence intensity of puncta over time shown in Panel c and d is compared to a first-order exponential curve. The plateau line represents fluorescence measurements from a nondestaining punctum (reproduced from see ref. 21 with permission from the Society of Neuroscience).

imaging chamber with a pipette. Bubble FM1-43 gently with carbogen applied locally using a micropipette (see Note 5).

3. Allow at least 2 min for the FM1-43 to load into synaptic terminals. Remove FM1-43 in high  $K^+$  ACSF and add 2 cc of 1 mM ADVASEP-7 (see Step 9b in Subheading 3.1) with a pipette. Bubble ADVASEP-7 gently with carbogen for 15 min. This will help to remove adventitious staining.
4. Focus the TPLSM on the striatum and capture images of fluorescent puncta (see Subheading 3.5 and Fig. 2).
5. After 9 baseline frames, continue TPLSM scanning and unload FM1-43 by superfusion with high  $K^+$  ACSF with 100  $\mu$ M ADVASEP-7 (see Step 9c in Subheading 3.1 and Note 6).

### **3.4. Loading and Unloading FM1-43 Using Cortical Stimulation**

1. Load FM1-43 specifically into corticostriatal terminals.
2. Using a fresh brain slice, attach bipolar electrodes to a manipulator and gently place the electrodes over cortical layers V–VI (see Note 7 and Fig. 1).
3. Stop ACSF perfusion, close the suction and carefully add 2 ml of FM1-43 (see Step 9d in Subheading 3.1) into the imaging chamber with a pipette. Bubble FM1-43 gently with carbogen (see Note 5).
4. Allow 10 min for the FM1-43 to penetrate the slice.
5. Load FM1-43 into corticostriatal presynaptic terminals using a 10 min train of 200  $\mu$ s, 400  $\mu$ A pulses at 10 Hz (see Figs. 1 and 2).
6. Stop stimulation. Without bumping the electrodes, carefully remove FM1-43 and add 1 mM ADVASEP-7 (see Step 9b in Subheading 3.1) with a pipette. Bubble ADVASEP-7 gently with carbogen, applied locally using a micropipette, for 2 min to remove adventitious staining.
7. Open suction drain and perfuse slices in ACSF containing 100  $\mu$ M ADVASEP-7 (see Step 9e in Subheading 3.1 and Note 6).
8. To prevent feedback synaptic transmission, expose sections to the pharmacological agents NBQX (AMPA receptor blocker), APV (NMDA receptor blocker), and CPCCOEt (to block metabotropic glutamate receptors).
9. Dopamine can be released by amphetamine or by local striatal stimulation. Likewise, receptor ligands can be bath-applied to detect alterations in FM1-43 destaining (see Fig. 1 and Note 8).
10. Focus the TPLSM on the striatum and capture images of fluorescent puncta (see Subheading 3.5 and Figs. 1 and 2).
11. After 9 baseline frames, continue TPLSM scanning and deliver 200  $\mu$ s, 400  $\mu$ A pulse trains to the cortex at 10 Hz for 10 min.

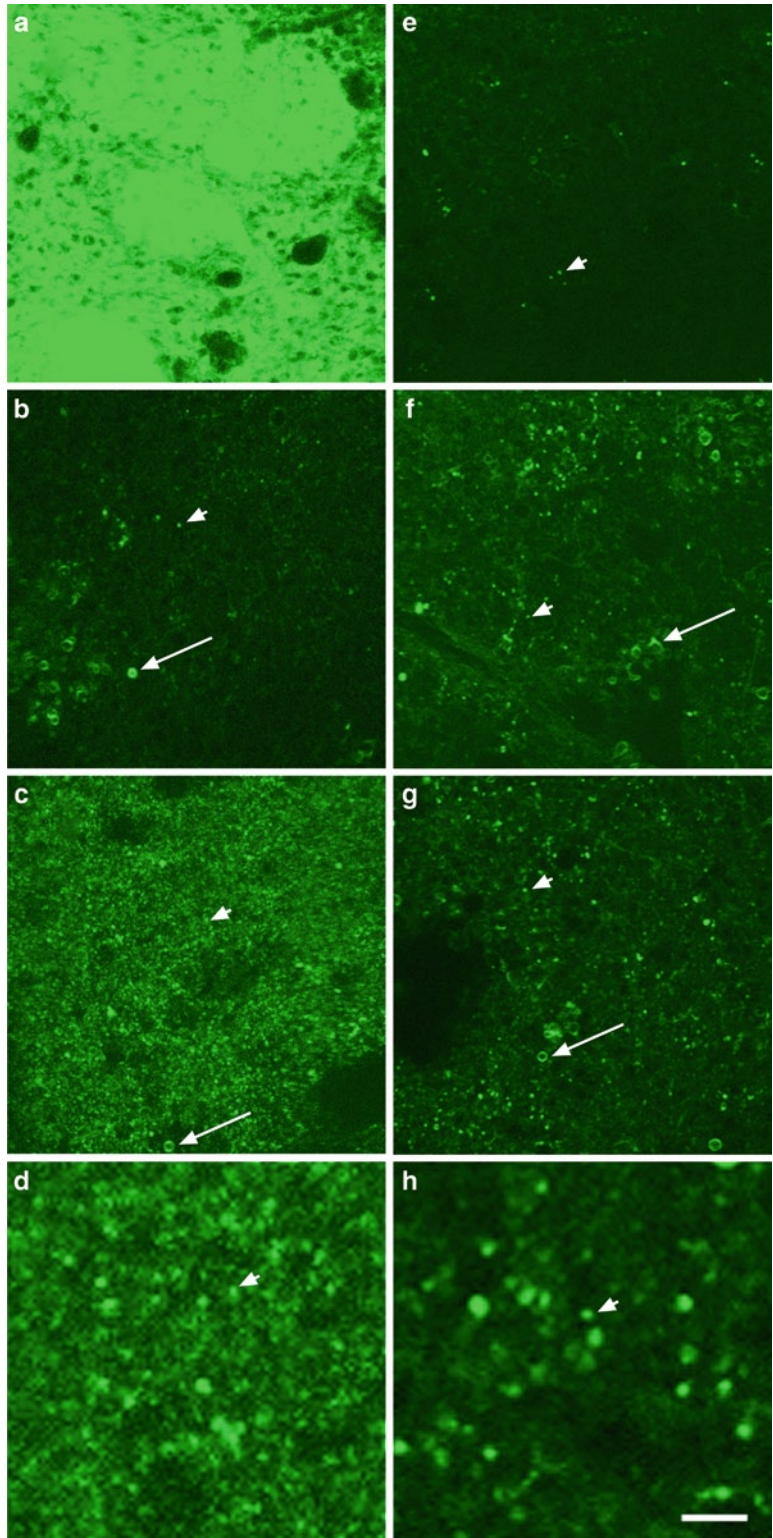


Fig. 2. Labeling striatal synaptic terminals with FM1-43. (a) TPLSM image of the dorsal striatum shows dramatic adventitious staining following incubation of a striatal slice in FM1-43 (8  $\mu$ M) for 10 min, followed by a 5 min wash in ACSF. The more darkly stained ovals are bundles of

### 3.5. Two-Photon Image Acquisition

1. Fluorescent corticostriatal terminals are visualized using a Zeiss TPLSM system. Images captured in 8-bit,  $123 \times 123 \mu\text{m}$  regions of interest (ROI) at  $512 \times 512$  pixel resolution and acquired at 21.5 second time intervals (see Notes 2 and 3).
2. During each time interval, obtain a  $z$ -series of five images, separated by  $1 \mu\text{m}$  in the  $z$ -plane. This will compensate for any minor  $z$ -axis shift.
3. Collect image stacks for 40 time intervals (3,600 s; 200 images). Perfuse with high  $\text{K}^+$  ACSF (see Step 5 in Subheading 3.3) or begin cortical stimulation at the start of the tenth time interval (see Step 11 in Subheading 3.4).

### 3.6. Data Analysis

1. Condense the image stack. Using the LSM 510 Browser software, align images in each  $z$ -series, condense the  $z$ -series stack with maximum transparency and export the 40 condensed images to a folder in tiff format (see Note 9).
2. Prepare the image stack for analysis (see Note 10).
3. Identify fluorescent puncta measuring  $0.5\text{--}1.5 \mu\text{m}$  in diameter (see Note 11).
4. Measure average FM1-43 fluorescence intensity of each punctum over the course of the time series (see Note 12).
5. Subtract the background fluorescence. Identify an area of tissue with no fluorescent puncta. Measure a sample of the slice background fluorescence for each time interval and subtract from the fluorescence intensity of each individual punctum.
6. Normalize the fluorescence intensity. For each punctum, normalize the time-dependent fluorescence intensity by the maximal puncta fluorescence just prior to the application of destaining stimulation (time frame 9).
7. Graph the normalized, background subtracted, intensity of each individual punctum using SigmaPlot software or another graphics software package. Active terminals are identified by the exponential decay of fluorescent intensity following stimulation (see Fig. 1 and Note 13). Reject any punctum that does

←

Fig. 2 (continued) corticofugal axons that course through the striatum. (b) When ADVASEP-7 (1 mM) was applied to the slice, most of the background staining was removed, leaving a few solitary puncta (*Arrow head*) and residual staining of larger diameter tube-like structures (*Arrow*), likely representing myelinated fibers or blood vessels. (c) FM1-43 in high  $\text{K}^+$  ACSF followed by ADVASEP-7 produced multiple fluorescent puncta. (d) Panel C was magnified 4 $\times$ , revealing puncta with diameters of  $\sim 0.5\text{--}2 \mu\text{m}$ . (e) FM1-43 was loaded into synaptic terminals using cortical bipolar stimulation at 10 Hz for 2 min. A progressively greater number of fluorescent puncta were seen after cortical stimulation for (f) 5 and (g) 10 min. (h) Magnifying panel G by 4 $\times$ , revealed puncta with diameters of  $\sim 0.5\text{--}2 \mu\text{m}$ . Bar,  $20 \mu\text{m}$  for panels a–c and e–g and  $5 \mu\text{m}$  for panels d and h.

not begin to destain following stimulation. Determine the halftime of fluorescence intensity decay during destaining ( $t_{1/2}$ ). Average the fluorescence intensity for all punctum across the time interval using Excel software or other software (see Fig. 1).

8. The fractional release of dye for each stimulation pulse can be determined using SigmaPlot software (see Note 14).

---

## 4. Notes

1. Mix solutions fresh each day. Alternatively, a 10× solution of salt (NaCl, KCl, NaHCO<sub>3</sub>, NaH<sub>2</sub>PO<sub>4</sub>, and HEPES) and a 10× solution of MgCl<sub>2</sub> and CaCl<sub>2</sub> can be prepared ahead of time and stored at 4°C for several weeks. The two 10× solutions are combined together with dH<sub>2</sub>O on the day of experiment and glucose is added. HEPES is used to help reduce slice edema and secondary movement artifact (26).
2. Several alternative TPLSMs can be used. We also use a Prairie Ultima TPLSM equipped with a titanium-sapphire laser (excitation 900 nm/emission 625 nm; Prairie, Middleton, WI), a Plan Fluor ×60 water-immersion objective (NA 1.2; Olympus) and an IBM computer with Prairie View software (Prairie). When using a Prairie TPLSM, images are captured in 16-bit, 75.2 × 75.2 μm ROI at 512 × 512 pixel resolution and acquired at 35-second intervals. An upright or inverted TPLSM can be used. In our experience, an upright microscope provides the best resolution (as the beam does not travel through a cover slip) while an inverted microscope affords a reduction in movement artifact. Whether inverted or upright, the TPLSM requires a stage platform and at least one electrode-holding micromanipulator.
3. FM1-43 dye has a single photon excitation maximum at 479 nm. The ideal laser excitation wavelength using two-photon imaging in these experiments should be determined to achieve adequate fluorescence signal yet maintain minimal laser power usage to reduce photo-bleaching of FM1-43. Optimal laser excitation wavelength and power (generally around ~10%) may vary between different set-ups. The pixel size (typically 0.22 μm) may vary, depending on chosen parameters. To further prevent photo-bleaching of the dye, minimize the intensity of mercury epifluorescence and bright field light and limit the duration of light source use in the presence of FM1-43.
4. Slice anchors are constructed from platinum wire and lycra threads with 1 mm spacing. An appropriately designed anchor will hold the brain slice in place while in the chamber bath and will

reduce the amount of slice movement during imaging. Fabricated slice anchors are also available from Warner Instruments.

5. Carbogen is applied locally using a small (1–10  $\mu\text{L}$ ) plastic micropipette. Attach a gas line to the micropipette. Place the tip of the pipette into the imaging bath, directing the flow of gas away from the brain slice. Minimize the gas flow so that the slice is not agitated.
6. ADVASEP-7 will help prevent recurrent endocytosis of FM1-43 dye into the recycling synaptic vesicles.
7. Robust placement of the stimulating electrode and imaging region are critical. Follow the referenced figure closely.
8. Amphetamine (10  $\mu\text{M}$ ) can be bath applied to release dopamine from nigrostriatal terminals (18). Dopamine (with other neurotransmitters) can also be released using a separate set of bipolar electrodes placed over the striatum, just adjacent to the imaging region. Striatal stimulation at 0.1 Hz produces little change in FM1-43 release while providing pulsatile dopamine efflux (18). To ensure equilibrium, the brain slice is generally exposed to pharmacological agents for 10 min before stimulation-mediated unloading (see Fig. 1).
9. Start the Zeiss LSM Image Browser and import the imaging file: name.lsm. To condense the z-stack, create a projection image: Process>Projections. The Projection window will open. Set the following parameters: Transparency=Maximum, Turning Axis=X, First Angle=0, Number of Projections=1, Difference Angle=0. Uncheck Single Time Index option. Choose “Apply”. The projection image with 40 slices will open in a new window. Export the condensed images to tiff files. File>Export>Set: Save as type “Tagged Image File 16-bit”. Label the files xxx-0.tif through xxx-39.tif.
10. Open the condensed image series in ImageJ software (v. 1.43u).
  - (a) Start ImageJ and import the condensed image files. File>Import>Image Sequence. Choose the first image of the stack “xxx-0.tif”. The Sequence Options dialog box opens; leave at the default settings. Choose “OK”.
  - (b) Set properties of the images acquired on the TPLSM. Image>Properties>Type “microns” as “Unit of Length” and assign the appropriate pixel width, height and depth (0.22  $\mu\text{m}$ ; see Note 3). Choose “OK”.
  - (c) Identify puncta by setting the threshold range of fluorescence intensity. Image>Adjust>Threshold. The Threshold window will open. The “Auto” function generally gives a good result. Select “Default”, “B&W”, and “Dark Background”. Choose “Apply”. If the “Convert to Mask” window opens check “Black Background” and OK. Close the Threshold window.

11. In ImageJ, select Analyze>Analyze Particles. Set size to 0.25–2.25. As nerve terminals are generally 0.5–1.5  $\mu\text{m}$  in diameter, the software requires the square of this range of values or 0.25–2.25. Adjust the circularity of desired objects to be identified, if desired. Select “Outlines” under the “Show” option. Check “Display Results”, “Clear Results”, “Add to Manager”, and “Exclude on Edges”. Choose “OK”. Choose “No” when asked to process all 40 images. A Drawing window opens. This shows the location of fluorescent puncta on the first image of the sequence.
12. Identify puncta over the remaining time points of the image sequence.
  - (a) In the “Results” window, Select Edit<Set Measurements. Select “Area”, “Mean Gray Value”, “Display Label”, and then “OK”.
  - (b) To ensure analysis of the time series, reselect the original image stack.
  - (c) Within the “ROI Manager” window, select all of the listed codes. Click the first code, shift bar then click on the last code. Select “More” and “Options”. Within the Options dialog box, select “Associate ‘show all’ ROIs with Slices” and then “OK”.
  - (d) Within the “ROI Manager” window, select “More” and click “Multi-Measure”. Check the option to “Measure All Slices” only. Choose “OK”.
  - (e) Save data as an excel spreadsheet. Results<File<Save As: name.xls and organize the data within Excel.
13. Nearness of fit to first-order kinetics is determined by comparing FM1-43 destaining with  $A=100*EXP(\ln(0.5)*t/t_{1/2})$  (an integrated form of the first-order kinetics equation,  $-d[A]/dt=k[A]$ ), using the square of the correlation coefficient ( $R^2$ ; see Fig. 1e).
14. Fractional release ( $f$ ) provides a measure of the change in fluorescent intensity over time. Calculate  $f$  for each punctum from  $\ln(F_1/F_2)/\Delta STIM$  (21, 27), where  $\ln$  is the natural logarithm,  $F_1$  and  $F_2$  are the fluorescent intensities at  $t_1$  and  $t_2$ , respectively, and  $\Delta STIM$  is the number of stimuli delivered during that period.

---

## Acknowledgments

This work was supported by DA07418, Picower and Parkinson’s Disease Foundations (DS) and by NS052536, NS060803, HD02274, University of Washington Vision Research Center and Children’s Hospital, Seattle, WA (NSB).

## References

1. Bamford, N. S., and Cepeda, C. (2009) The Corticostriatal Pathway in Parkinson's Disease, in *Cortico-Subcortical Dynamics in Parkinson's Disease* (Tseng, K. Y., Ed.), pp 87–104, Humana Press, New York.
2. Graham, R. C., Jr., and Karnovsky, M. J. (1965) The histochemical demonstration of uricase activity, *J Histochem Cytochem* **13**, 448–453.
3. Holtzman, E., Freeman, A. R., and Kashner, L. A. (1971) Stimulation-dependent alterations in peroxidase uptake at lobster neuromuscular junctions, *Science* **173**, 733–736.
4. Wilcox, M., and Franceschini, N. (1984) Illumination induces dye incorporation in photoreceptor cells, *Science* **225**, 851–854.
5. Lichtman, J. W., Wilkinson, R. S., and Rich, M. M. (1985) Multiple innervation of tonic endplates revealed by activity-dependent uptake of fluorescent probes, *Nature* **314**, 357–359.
6. Zhang, Q., Cao, Y. Q., and Tsien, R. W. (2007) Quantum dots provide an optical signal specific to full collapse fusion of synaptic vesicles, *Proc Natl Acad Sci USA* **104**, 17843–17848.
7. Miesenbock, G., De Angelis, D. A., and Rothman, J. E. (1998) Visualizing secretion and synaptic transmission with pH-sensitive green fluorescent proteins, *Nature* **394**, 192–195.
8. Voglmaier, S. M., Kam, K., Yang, H., Fortin, D. L., Hua, Z., Nicoll, R. A., and Edwards, R. H. (2006) Distinct endocytic pathways control the rate and extent of synaptic vesicle protein recycling, *Neuron* **51**, 71–84.
9. Gubernator, N. G., Zhang, H., Staal, R. G., Mosharov, E. V., Pereira, D. B., Yue, M., Balsanek, V., Vadola, P. A., Mukherjee, B., Edwards, R. H., Sulzer, D., and Sames, D. (2009) Fluorescent false neurotransmitters visualize dopamine release from individual presynaptic terminals, *Science* **324**, 1441–1444.
10. Betz, W. J., and Bewick, G. S. (1992) Optical analysis of synaptic vesicle recycling at the frog neuromuscular junction, *Science* **255**, 200–203.
11. Betz, W. J., Mao, F., and Smith, C. B. (1996) Imaging exocytosis and endocytosis, *Curr Opin Neurobiol* **6**, 365–371.
12. Harata, N., Ryan, T. A., Smith, S. J., Buchanan, J., and Tsien, R. W. (2001) Visualizing recycling synaptic vesicles in hippocampal neurons by FM 1–43 photoconversion, *Proc Natl Acad Sci USA* **98**, 12748–12753.
13. Rhee, M., and Davis, P. (2006) Mechanism of uptake of C105Y, a novel cell-penetrating peptide, *J Biol Chem* **281**, 1233–1240.
14. Ryan, T. A., Smith, S. J., and Reuter, H. (1996) The timing of synaptic vesicle endocytosis, *Proc Natl Acad Sci USA* **93**, 5567–5571.
15. Stevens, C. F., and Tsujimoto, T. (1995) Estimates for the pool size of releasable quanta at a single central synapse and for the time required to refill the pool, *Proc Natl Acad Sci USA* **92**, 846–849.
16. Pothos, E. N., Davila, V., and Sulzer, D. (1998) Presynaptic recording of quanta from midbrain dopamine neurons and modulation of the quantal size, *J Neurosci* **18**, 4106–4118.
17. Zakharenko, S. S., Zablow, L., and Siegelbaum, S. A. (2001) Visualization of changes in presynaptic function during long-term synaptic plasticity, *Nat Neurosci* **4**, 711–717.
18. Bamford, N. S., Zhang, H., Schmitz, Y., Wu, N. P., Cepeda, C., Levine, M. S., Schmauss, C., Zakharenko, S. S., Zablow, L., and Sulzer, D. (2004) Heterosynaptic dopamine neurotransmission selects sets of corticostriatal terminals, *Neuron* **42**, 653–663.
19. Bamford, N. S., Zhang, H., Joyce, J. A., Scarlis, C. A., Hanan, W., Wu, N. P., Andre, V. M., Cohen, R., Cepeda, C., Levine, M. S., Harleton, E., and Sulzer, D. (2008) Repeated exposure to methamphetamine causes long-lasting presynaptic corticostriatal depression that is renormalized with drug readministration, *Neuron* **58**, 89–103.
20. Bamford, N. S., Robinson, S., Palmiter, R. D., Joyce, J. A., Moore, C., and Meshul, C. K. (2004) Dopamine modulates release from corticostriatal terminals, *J Neurosci* **24**, 9541–9552.
21. Joshi, P. R., Wu, N. P., Andre, V. M., Cummings, D. M., Cepeda, C., Joyce, J. A., Carroll, J. B., Leavitt, B. R., Hayden, M. R., Levine, M. S., and Bamford, N. S. (2009) Age-dependent alterations of corticostriatal activity in the YAC128 mouse model of Huntington disease, *J Neurosci* **29**, 2414–2427.
22. Kay, A. R., Alfonso, A., Alford, S., Cline, H. T., Holgado, A. M., Sakmann, B., Snitsarev, V. A., Stricker, T. P., Takahashi, M., and Wu, L. G. (1999) Imaging synaptic activity in intact brain and slices with FM1–43 in *C. elegans*, lamprey, and rat, *Neuron* **24**, 809–817.
23. Winterer, J., Stanton, P. K., and Muller, W. (2006) Direct monitoring of vesicular release and uptake in brain slices by multiphoton excitation of the styryl FM 1–43, *Biotechniques* **40**, 343–351.

24. Mainen, Z. F., Maletic-Savatic, M., Shi, S. H., Hayashi, Y., Malinow, R., and Svoboda, K. (1999) Two-photon imaging in living brain slices, *Methods* **18**, 231–239, 181.
25. Franklin, K. B. J., and Paxinos, G. (1997) *The Mouse Brain in Stereotaxic Coordinates*, Academic Press, San Diego.
26. MacGregor, D. G., Chesler, M., and Rice, M. E. (2001) HEPES prevents edema in rat brain slices, *Neurosci Lett* **303**, 141–144.
27. Isaacson, J. S., and Hille, B. (1997) GABA(B)-mediated presynaptic inhibition of excitatory transmission and synaptic vesicle dynamics in cultured hippocampal neurons, *Neuron* **18**, 143–152.